



Mass-Conservation Increases Robustness in Stochastic Reaction-Diffusion Models of Cell Crawling

Eduardo Moreno and Sergio Alonso*

Department of Physics, Universitat Politècnica de Catalunya, Barcelona, Spain

The process of polarization determines the head and tail of single cells. A mechanism of this kind frequently precedes the subsequent cell locomotion and it determines the direction of motion. The process of polarization has frequently been described as a reaction-diffusion mechanism combined with a source of stochastic perturbations. We selected a particular model of amoeboid cell crawling for the motion of *Dictyostelium discoideum* and studied the interplay between pattern formation and locomotion. Next, we integrated the model in a two-dimensional domain considering the shape deformations of the cells in order to characterize the dynamics. We observed that the condition of pattern formation is finely tuned and we propose a modification based on the use of a mass-conservation constraint to substantially increase the robustness of the mathematical model.

Keywords: bistability, stochastic partial differential equations, pattern formation, *Dictyostelium discoideum*, cell polarization, amoeboid motion

OPEN ACCESS

Edited by:

Luis Diambra,
National University of La Plata,
Argentina

Reviewed by:

Satoshi Sawai,
The University of Tokyo, Japan
M. N. Kuperman,
Bariloche Atomic Centre (CNEA),
Argentina

*Correspondence:

Sergio Alonso
s.alonso@upc.edu

Specialty section:

This article was submitted to
Biophysics,
a section of the journal
Frontiers in Physics

Received: 23 February 2022

Accepted: 12 April 2022

Published: 28 April 2022

Citation:

Moreno E and Alonso S (2022) Mass-Conservation Increases Robustness in Stochastic Reaction-Diffusion Models of Cell Crawling.
Front. Phys. 10:881885.
doi: 10.3389/fphy.2022.881885

1 INTRODUCTION

An intensive use of physical and mathematical theories on pattern formation in extended systems [1, 2], gave rise to valuable arguments to explain the formation of certain biological structures. Such mathematical mechanisms have permitted the modeling of processes on very different spatial and temporal scales: from the formation of the skin in fishes [3], to the definition of the direction in embryonic developing [4]. Such mechanisms have to be robust to small changes of parameters in order to be reliable. Robustness is a generic feature of living cells. It ensures that specific cellular functions are maintained despite external and internal change on the conditions. System control and feedback control are some of the characteristic mechanisms that allow robustness [5, 6].

Cell migration is an example of robust phenomenon that is present both in prokaryotic and eukaryotic cells. Living cells migrate to perform different tasks such as food targeting, wound healing and immune response. Independently of the presence of an external signal, before moving, cells need to define the direction to follow. To do so, they first define the front and the back of the cell. The process of formation of a polar direction inside a single cell is commonly known as cell polarization [7] and it is a typical example of pattern formation at the cellular level [8].

Several mathematical models have been developed to explain polarization of single eukaryotic cells [9–11]. Some models rely on a local excitation, which, combined with global inhibition makes the cell respond to external gradients [12], others rely on the accumulation of a certain biochemical components to guide the motion of the single cells [13]. The accumulation responsible for this second mechanism is frequently combined with a conservation constraint because the process of polarization is fast in comparison to the production of new biochemical components. With this

restriction, the mechanism of pattern formation inside living cells, together with the constraint of mass conservation, is analogous to a process of coarsening of the initial nucleus of components [14] and gives rise to phase separation [15] and to models of pattern formation [16]. Several simple models of intracellular pattern formation have appeared including the conservation restriction [13, 17, 18].

Once the axes and direction of movement are defined in amoeboid cells, small projections (defined as protrusions) are formed at the membrane of the cells [19]. These projections, which extend and retract periodically, are responsible for pushing the cell, and therefore, to move in the typical amoeboid motion. *Dictyostelium discoideum* is a species of soil-dwelling amoeba, frequently employed to characterize amoeboid locomotion. Inside the amoeba several signaling events are triggered, for example the activation of the Ras proteins and PI3K enzymes and accumulation of *PIP*₃ at the front of the cell, while activation of PTEN and myosin occur at the rear of the cell [20, 21]. Membrane areas where the protrusion activity is greater are typically characterized by the presence of Ras-GTP protein patches [22]. The appearance of Rac regions around the membrane with high protrusion activity [23, 24] has been observed in the slime mold organism *Dictyostelium discoideum*, where it is related to cytoskeletal dynamics [25].

A reaction-diffusion model with bistable dynamics is one of the common models of cell motility and particularly employed for *Dictyostelium discoideum*. Some dimensional bistable models are based on the formation of a finite lifetime and localized patches of high protein concentration [26, 27] while others are based on membrane dynamics of moving connected points [28]. Bistable conditions for cellular processes can be obtained by the coupling of a mass control regulating condition in the biochemical components present around the cytosol and the membrane of the cell, for example proteins, phospholipids and enzymes [13, 16, 29].

A common technique to model pattern formation inside a cell and the shape evolution of the membrane is the addition of a phase field with a sharp interface to distinguish the interior and exterior of the cell. This field maintains the correct boundary conditions while the borders are moving [30]. Some studies have applied phase field modeling to study keratocyte motility [31–33] and amoeboid motility [34] which can be divided into diffuse and persistent migration depending on the starvation level [35, 36]. There are also some intermediate cases observed in *Dictyostelium discoideum* cells for certain types of genetic variants [37] which have also been modelled with a phase field and variation of some parameters [38–40]. Other properties of *Dictyostelium discoideum* cells modeled employing a phase field are the viscoelasticity of the cells [41] and cell division [42]. Finally, we would like to mention that interactions among cells can also be considered for keratocyte [43, 44] and amoeboid cells [45].

Here, first, we transform a one dimensional model of the polarization at the membrane of a single *Dictyostelium discoideum* cell [23] into a two-dimensional domain for the waves in the basal membrane, in contact with the surface, using an additional phase field for the shape of the cell. We observe a strong dependence of the numerical dynamics on the explicit

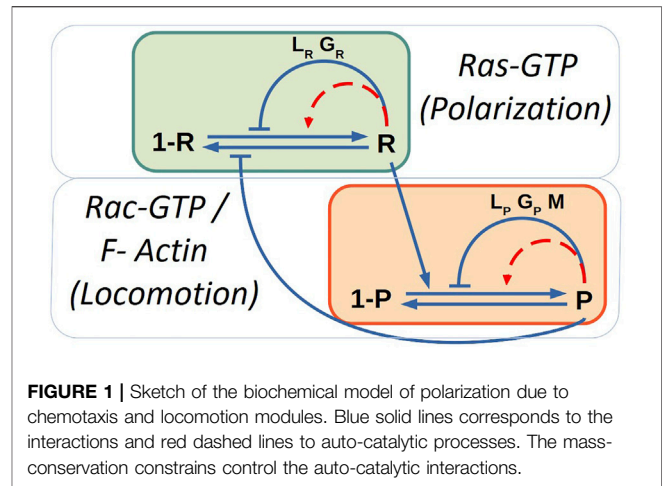


FIGURE 1 | Sketch of the biochemical model of polarization due to chemotaxis and locomotion modules. Blue solid lines corresponds to the interactions and red dashed lines to auto-catalytic processes. The mass-conservation constrains control the auto-catalytic interactions.

parameter values of the original model. Cell motion occurs only in a small window of parameter values, which indicates that the model is not robust to small variations of the parameters. Therefore, we propose a constraint on the conservation of a component of the signal pathway, controlling the autocatalytic mechanism, in order to increase the robustness of the model in representing changes in parameter values [46]. Similar types of conservation have previously been employed in other models of motion of *Dictyostelium discoideum* cells [34, 38, 47, 48], and we show here that a constraint of this kind is an useful and reasonable condition to systematically increase the robustness of the crawling mechanism, increasing the window of parameter values allowing cell migration.

2 MATERIALS AND METHODS

2.1 Biochemical Model for Ras Activation and Pseudopod Extension

Biochemical components inside the *Dictyostelium discoideum* amoeba self-organized to follow chemical signals in the exterior by the accumulation of Ras-GTP in the front of the cell. Next, F-actin molecules accumulates also at the front triggering push of the cytoskeleton and the motion of the amoeba.

We investigate a simple reaction-diffusion model [23] for Ras-GTP (R) patches that consists on the next partial differential equation:

$$\frac{\partial R}{\partial t} = (1 - R) \left(k_0 + k_1 S + \frac{k_2 R^{n_1}}{R^{n_1} + K_R^{n_1}} - k_3 G_R - k_4 L_R \right) - \frac{k_5 R}{1 + k_6 P} + D_R \nabla^2 R + \xi_R(\mathbf{x}, t), \tag{1}$$

where we have a basal production, the stimulation production R by local occupied receptor S, an autocatalytic stimulation of R, an inhibition R by global and local inhibitors (G_R and L_R), the degradation of R, the diffusion of R and, a Gaussian spatio-temporal distributed white noise $\xi_R(\mathbf{x}, t)$ with zero mean $\langle \xi_R(\mathbf{x}, t) \rangle = 0$ and correlation $\langle \xi_R(\mathbf{x}, t) \xi_R(\mathbf{x}', t') \rangle = 2\sigma_R \delta(\mathbf{x} - \mathbf{x}') \delta(t - t')$. The external S can

significantly increase the response of Ras [23], see diagram in **Figure 1**, therefore, we keep here $S = 0$.

The variables L_R and G_R correspond, respectively, to local and global inhibitors of R:

$$\frac{\partial G_R}{\partial t} = k_7 \bar{R} - k_9 G_R, \tag{2}$$

$$\frac{\partial L_R}{\partial t} = (1 - L_R)k_{10}R - k_{11}L_R + D_{LR}\nabla^2 L_R; \tag{3}$$

where both are produced by R and degrade, and only the local inhibitor diffuses. Note that the quantity \bar{R} corresponds to the spatial average in the whole space of the field R.

At the same time we included a quantity related to the formation of protrusions (P) such as F-actin and Rac-GTP molecules; see diagram in **Figure 1**. This variable P was coupled with its respective inhibitors:

$$\frac{\partial P}{\partial t} = (1 - P)\left(k_{12} + k_{13}R + \frac{k_{14}P^{m_2}}{P^{m_2} + K_P^{m_2}} + \frac{k_{15}M^{m_3}}{M^{m_3} + K_M^{m_3}} - k_{16}G_P - k_{17}L_P\right) - k_{18}P + D_P\nabla^2 P + \xi_P(\mathbf{x}, t), \tag{4}$$

where we have a basal production, the stimulation production by R, an autocatalytic stimulation of P, a production by an extra term M, an inhibition of P by global and local inhibitors (G_P and L_P), the degradation of P, the diffusion of P and, a Gaussian spatio-temporal distributed white noise $\xi_P(\mathbf{x}, t)$ with zero mean $\langle \xi_P(\mathbf{x}, t) \rangle = 0$ and correlation $\langle \xi_P(\mathbf{x}, t)\xi_P(\mathbf{x}', t') \rangle = 2\sigma_P\delta(\mathbf{x} - \mathbf{x}')\delta(t - t')$.

Similar to the previous set of equations, the variables L_P and G_P correspond, respectively, to local and global inhibitors of P:

$$\frac{\partial G_P}{\partial t} = k_{19}\bar{P} - k_{20}G_P, \tag{5}$$

$$\frac{\partial L_P}{\partial t} = (1 - L_P)k_{21}P - k_{22}L_P + D_{LP}\nabla^2 L_P; \tag{6}$$

where both are produced by P and degrade, and only the local inhibitor diffuses. Note that the quantity \bar{P} corresponds to the spatial average in the whole space of the field P.

Finally, the model takes into account the inclusion of a variable of memory (M) which is coupled with P; this variable stimulates the formation of new protrusion zones and represents the results observed in some experiments:

$$\frac{\partial M}{\partial t} = k_{23}P - k_{24}M + D_M\nabla^2 M. \tag{7}$$

which is produced by P, degrades and diffuses. The memory term is related to the probability of identifying when and where the signaling cascade is activated to generate new pseudopods. At a molecular level, such term is identified with the mechanisms of how information is collected, stored and used to bias future pseudopods [49, 50].

A more exhaustive description of the model is shown in the original study [23]. However, note that the noise description in the original study was different and we have adapted to an equivalent description based on physical derivations of stochastic fluctuations [51]; for more details see **Supplementary Material**.

One dimensional simulations were made using periodic boundary conditions in a grid of 120 points. The cell was considered as circular and having a radius of $6.25 \mu m$. The pixel size for this case was set at $\Delta x = 0.32 \mu m$ and the time step $\Delta t = 0.03 s$. The definition and the value of the parameters of the model can be found in **Supplementary Table S1**.

2.2 Physical Phase Field Model for Cell Shape Deformations

The original model did not include deformable cells. Therefore, we expanded the model to 2D geometry and introduced an auxiliary phase field ϕ with the purpose of describing the evolution of the cell shape. The use of a phase field permits a smooth variation between the values of $\phi = 1$ inside and $\phi = 0$ outside of the cell.

The phase field equation is the result of a force balance involving several types of forces of different origins acting in the cell body. The equation for the phase field is as follows

$$\tau \frac{\partial \phi}{\partial t} = \gamma \left(\nabla^2 \phi - \frac{G'(\phi)}{\epsilon^2} \right) - \beta \left(\int \phi dA - A_0 \right) |\nabla \phi| + \alpha \phi P |\nabla \phi|, \tag{8}$$

The first term on the right side in **Eq. 8** is related to the surface energy of the cell membrane, where γ is the surface tension and $G(\phi) = 18\phi^2(1 - \phi)^2$ is a double well potential. The second term keeps the area close to the value of A_0 . And the third term represents the active force generated by the Rac-GTP (P) molecules when pushing on the cell membrane [34]. The inclusion of the phase field permits to mimic the shape of the ventral membrane of crawling cells.

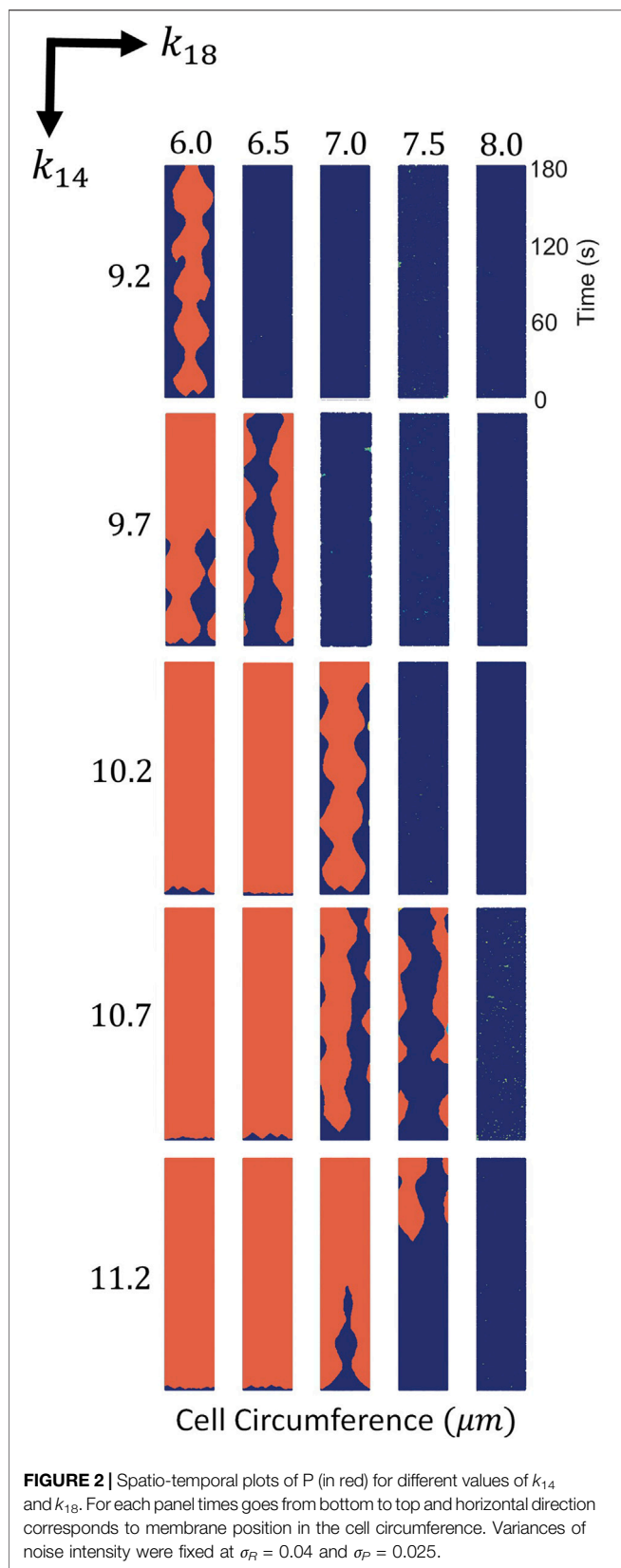
We consider a deformable cell of $122 \mu m^2$ in area corresponding to a circle with radius equal to $6.25 \mu m$. The pixel size used was the half as in the 1D case $\Delta x = \Delta y = 0.16 \mu m$. Also, to increase accuracy, the time discretization was reduced to $\Delta t = 0.003s$. We integrated **Eqs 1–8** using periodic boundary conditions and standard finite differences. The rest of parameters are as displayed in **Supplementary Table S1**.

2.3 Mathematical Description of the Mass-Conservation Constraint

The mathematical model represented in **Eqs 1–7** has several conservation terms which affect the dynamics of the system; see for example **Eqs.2–5**. However, we further modify the original model to include a new feedback through parameters k_{14} to create a more robust model by the control of the bistable properties, which are discussed in following sections. Therefore, the parameter k_{14} is dynamically controlled depending on the total amount of the protein of the inducer P at the cell. A new control term related to k_{14} is incorporated, following previous similar approaches in simple models [32, 38, 47]:

$$k_{14} = k_{14}^* + \eta(\bar{P} - C_P), \tag{9}$$

where k_{14}^* is a new constant that take the values of the original value of k_{14} . It is important to note that the new constrain



precludes the cell to be fully covered with the component P or emptying of the component P . Both extreme conditions are rare during cell crawling.

Parameter C_P is the target value of the fraction of the cell area occupied by patches of pseudopod inducer P . When, the total concentration \bar{P} is larger (lower) than C_P the parameter value of k_{14} is larger (lower) than k_{14}^* and the bistable conditions implies the reduction (increase) of the \bar{P} . It corresponds to a feedback control of the parameter to keep a particular stable solution in Eq. 9. Note that for $\eta = 0$ we recover the original model.

3 RESULTS

3.1 Mechanism of Cell Motion in the Mathematical Model Is Based in Stochastic Generation of Patches

In a one-dimensional system, mimicking the membrane of a crawling cell, the generation of a single local patch of high biochemical concentration is equivalent to cell polarization. A stable domain in a specific location of the membrane is related with actin accumulation and produces persistent motion of the cell in that direction. The random appearance and disappearance of small domains is related with amoeboid motion, where two or three pseudopods compete for a certain time. The alternation of direction gives rise to random motion of the virtual cell.

Stochastic reaction-diffusion equations, as in Eqs 1–7, and previously developed [23], can be numerically integrated into a one-dimensional domain as in the original study, where kymographs are shown for a certain window of parameter values.

If we vary the parameters k_{14} and k_{18} , we obtain the phase diagram; see Figure 2. For large values of k_{14} and small values of k_{18} the membrane is completely covered by P , while for small values of k_{14} and large values of k_{18} the concentration of P strongly decreases. Locomotion is, therefore, expected for intermediate values of these two parameters as shown in Figure 2. For the evaluation of the mechanism of the simulations shown in Figure 2, we fixed the stochastic source of perturbations of the additive noises in Eqs 1–7 to $\sigma_R = 0.04$ and $\sigma_P = 0.025$.

3.2 Mechanism of Cell Motion Is Based in Bistability

For the evaluation of the mechanism of pattern formation we found the stationary solutions for the deterministic version of Eqs 1–7 by removing the additive noise. We have slowly increased the parameter k_{14} by small intervals (0.05 s^{-1}) and integrated the model for a considerable amount of time to permit the model reach the equilibrium (180 s). Subsequent increase of the parameter permits the observation of the evolution of the stationary value of P by obtaining a value for P in every interval in k_{14} ; see Figure 3A. Once the system of equations

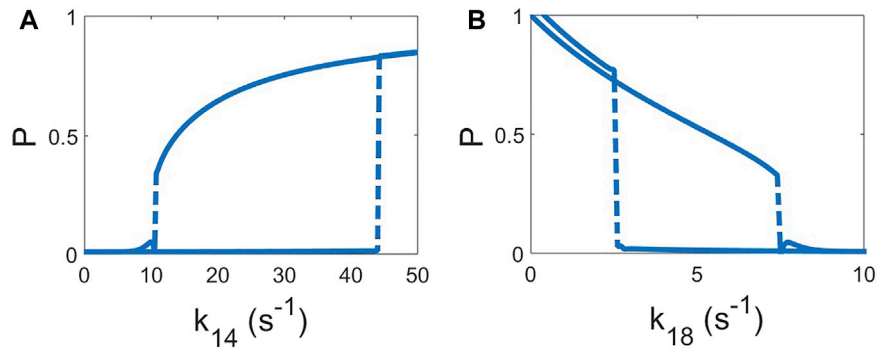


FIGURE 3 | Hysteresis curves of the deterministic model ($\sigma_R = 0$ and $\sigma_P = 0$). The value of the homogeneous solution of P is shown as function of the parameter increasing and, subsequently, decreasing of k_{14} , keeping $k_{18} = 7 \text{ s}^{-1}$ (**A**) and k_{18} keeping $k_{14} = 10.2 \text{ s}^{-1}$ (**B**). Increase and decrease of the both parameters are done by steps of 0.05 s^{-1} and, after each step, permitting to relax to the new solution for 180 s.

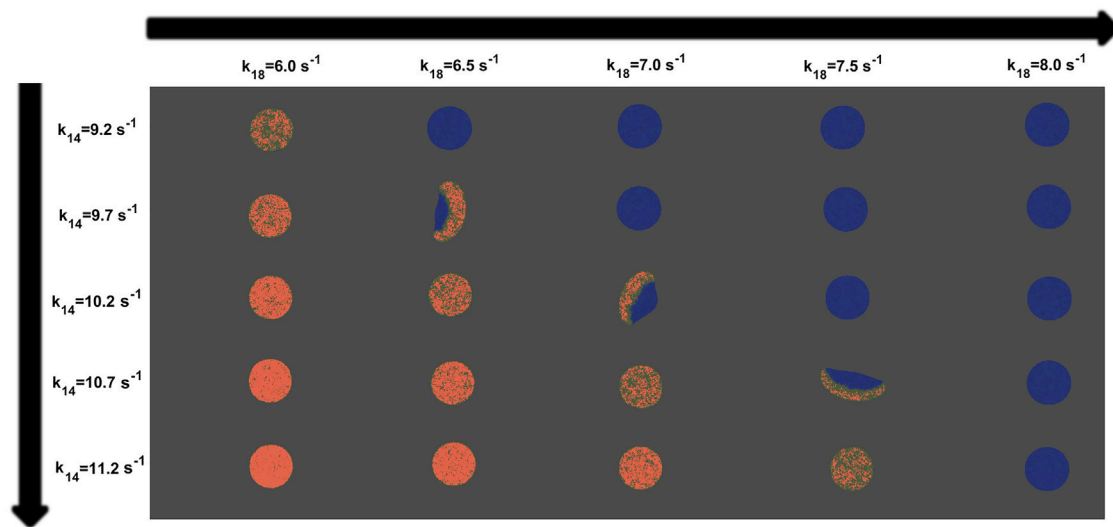


FIGURE 4 | Snapshots of the virtual cells showing P (in red) obtained from computer simulations and applying the phase field technique to the model for different values of k_{14} and k_{18} . Variances of noise intensity were fixed at $\sigma_R = 0.04$ and $\sigma_P = 0.025$. The rest of them are consistent with **Supplementary Table S1**.

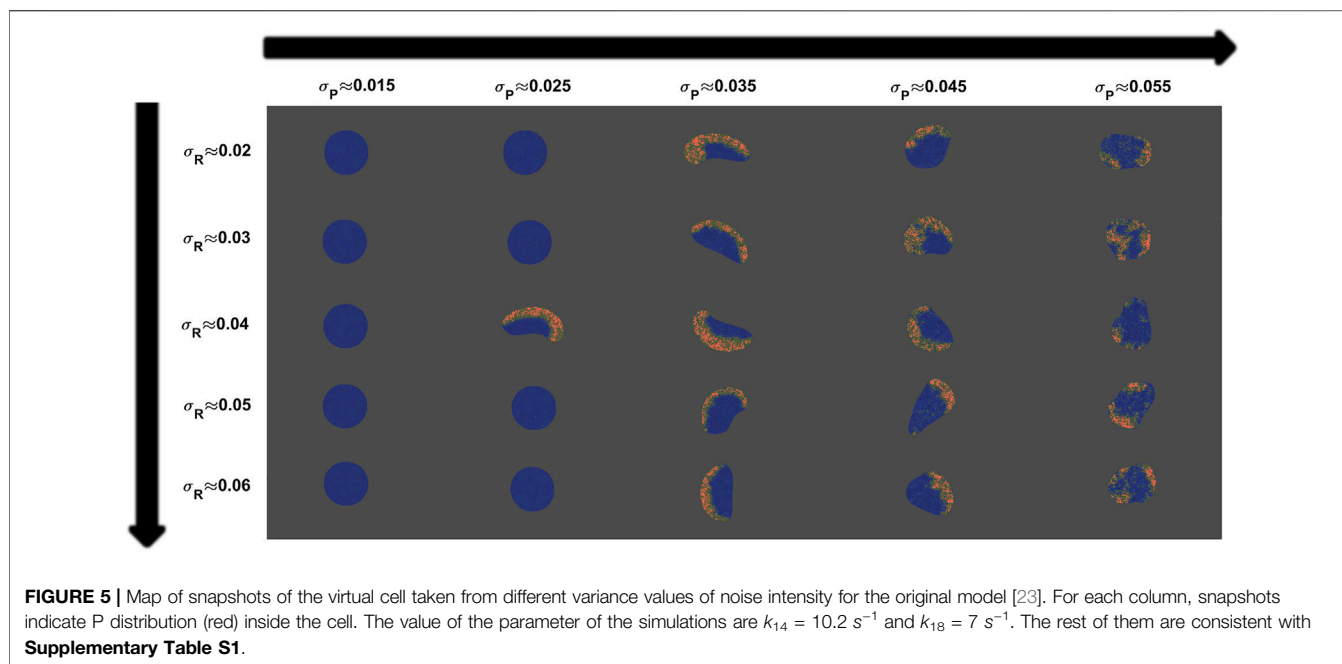
saturated to a certain value of $P \sim 0.75 - 0.80$ we stopped and reduced the value of k_{14} , giving rise to a hysteresis cycle; see **Figure 3A**. The hysteresis cycle shows that the system actually is bistable for certain window of parameter values. Equivalent dynamics of P can be observed under a similar change in k_{18} ; see **Figure 3B**. Therefore for low and large values of k_{14} and k_{18} there is a single stable solution and for intermediate values the model shows bistability.

It is known that the combination of a bistable dynamics with an appropriate noise intensity produces the formation of localized patches in reaction-diffusion equations [52, 53]. This formation is the mechanism responsible for the formation of localized domains of P. The localized pattern observed in **Figure 2** is not due to excitable dynamics but rather to a delicate equilibrium between bistable dynamics and noise.

3.3 Stochastic Bistability Provides a Mechanism of Cell Crawling Motion in Two Dimensional Systems

For the coupling of the polarization mechanism to the cell motion we used a phase field. This additional field is employed for the definition of the interior of the cell. In this case, the two dimensional phase field permits the use of different biochemical concentrations in the ventral membrane of a crawling cell.

The extension of the stochastic reaction-diffusion described in the previous section to two dimensions permits numerical simulations of the shape of the crawling cell and the corresponding motion responding to the dynamics of the patches. In **Figure 4** we showed snapshots of the *in silico* cells with the parameter values corresponding to the values shown in **Figure 2**. We reproduced the dynamics expected from the one



dimensional simulations, and the crawling dynamics can be clearly studied. Again, for high values of parameter k_{14} and small values of k_{18} the concentration of P is mostly high and homogeneously distributed along the membrane; see **Figure 4**. On the other hand, in the opposite limit, for small values of k_{14} and high values of k_{18} the concentration of P disappears from the ventral membrane. However, for a small window of values of the parameters the cell moves and inspects the surrounding region. The shape of the resulting cell depends on the particular realization and the parameter values; in the snapshots shown in **Figure 4** we obtain fan-shaped cells, a typical mode of *Dictyostelium discoideum* cell crawling [37].

The dependence of locomotion on the parameters k_{14} and k_{18} is strong as shown in **Figure 4**. Persistent motion is observed only for an intermediate window of values of the two parameters. For very small or very large amounts of \bar{P} cells do not move. Such quantity is determined by the parameters k_{14} and k_{18} , and small changes on their values prevent the cell motion, making the whole model non-robust.

3.4 Noise Intensities Determine the Type of Motion

The variation of the type of cell motion is determined by the intensity of the noise. Low levels of both noises do not permit the formation of the domains of P needed to give rise to cell movement; see **Figure 5**. As we increase the amplitude of noise for P, we reach a single domain that fills the front part of the cell and persistent motion is shown; see middle column and right hand snapshots in **Figure 5**. This type of motion is reminiscent of the fan-shaped amoeboid cells previously reported [37] and also reproduced with simpler models [38]. An increase in the noise intensity produces an increase in the appearance and disappearance of pseudopods and therefore a transition to amoeboid movement; see fifth column in **Figure 5**

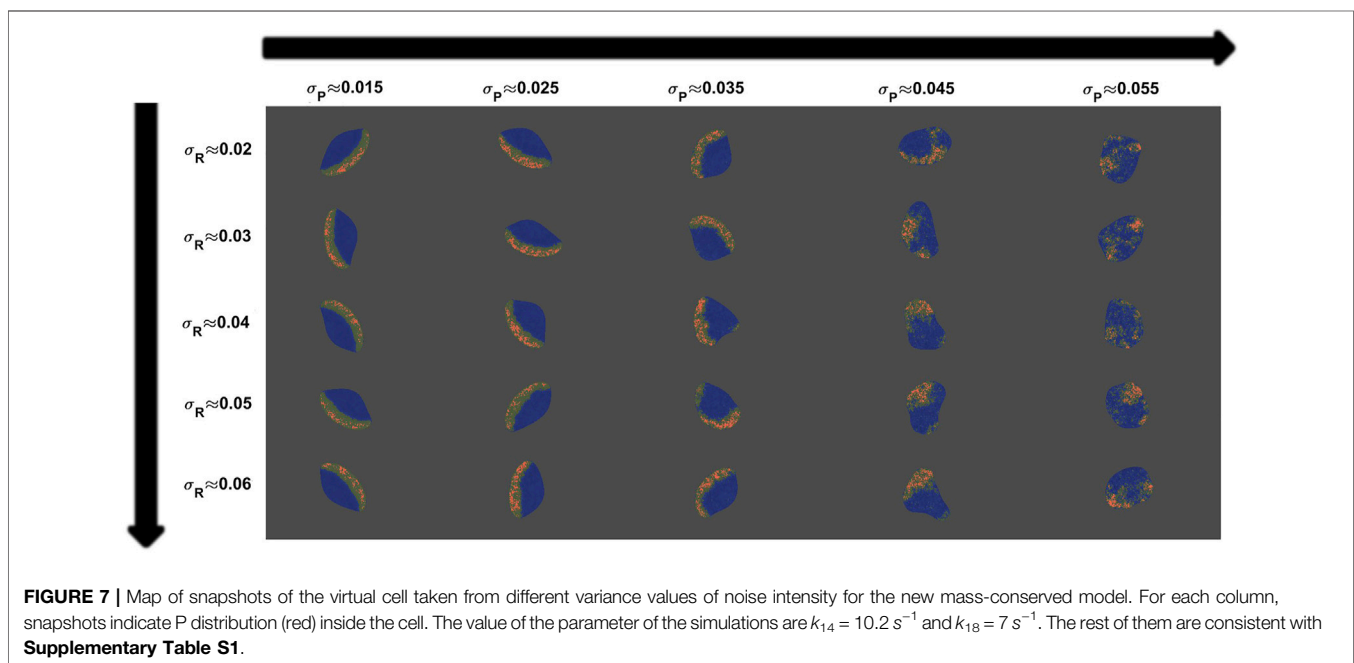
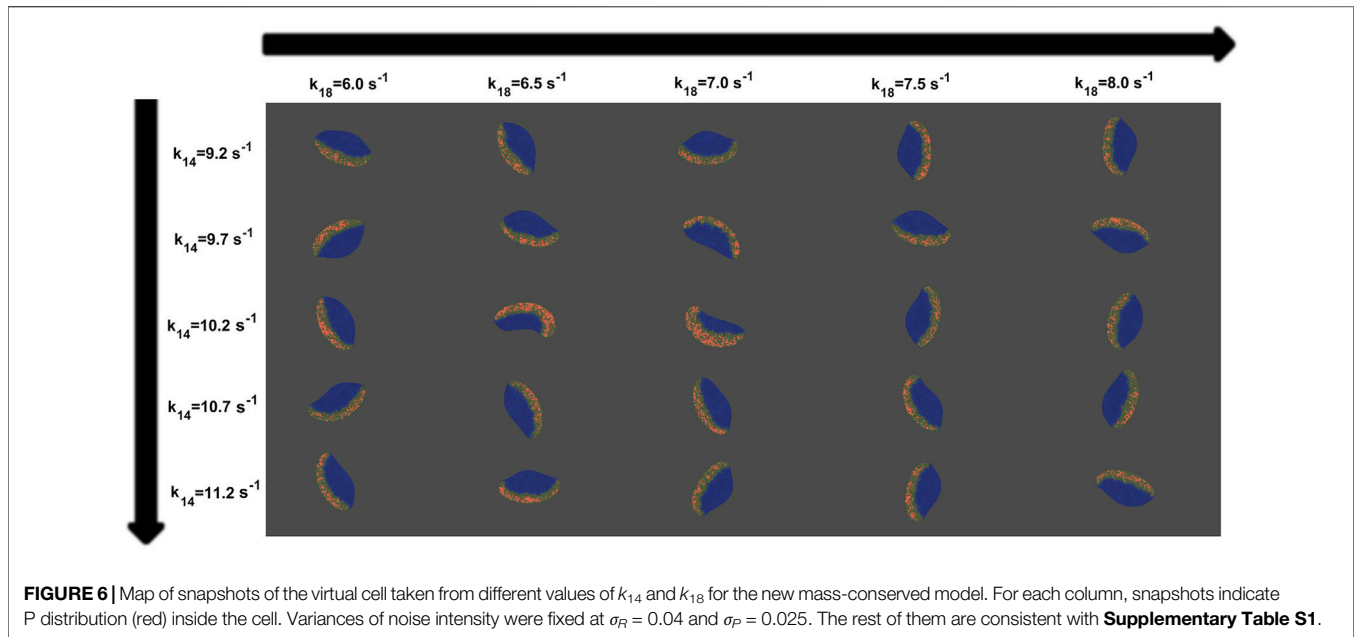
for higher noise intensities. There are some noise intensities which produce patterns and dynamics similar to the characteristic patterns observed in the experiments, however, as previously mentioned, and shown in **Figure 4**, small variations in the parameter values k_{14} and k_{18} may completely change the movement dynamics.

3.5 Inclusion of Mass-Conservation Constrain Qualitatively Increases Robustness

In order to reduce the high sensitivity of the appearance of motion on the parameter values, we included a conservation constraint on the total inducer P, see **Eq. 9**, in the biochemical rates responsible for the bistable transition in **Eq. 4**. Following similar previous approaches [34, 47], we included this conservation as a global feedback condition in the reaction-diffusion equations of the model, see **Section 2.3**.

In **Figure 6**, we show several realizations incorporating the conservation constraint of P proteins, for different k_{14} and k_{18} parameter. A direct comparison can be made with the results displayed in **Figure 4** showing the effects of the inclusion of the mass conservation feedback. Results in **Figure 6** show that for a wide range of parameter values, the variation of the parameters does not affect either the bistability of the model or the quantity of inducer P inside the cell phase field, which was kept constant. The inclusion of this global condition permits the use of a larger range of parameter values, increasing the robustness of the mechanism in comparison with the original model.

The shape and type of motion were affected by the noise intensity. Using the same parameters of **Figure 5** we studied the effects of varying the noise variance in the new mass-conserved model. When the noise intensity related to the pseudopod inducer P increases, changes the shape from persistent fan-



shape to random amoeboid phenotype, see **Figure 7**. This change is present because while small values of σ_P generates less blurred patches, an increment of σ_P drives the opposite effect, the appearance of more blurred and distributed patches for P.

3.6 Inclusion of Mass-Conservation Constrain Quantitatively Increases Robustness

We measured the speed of the resulting cells for different parameter conditions for the original and the new mass-

conserved models. We observed that the dynamics of the simulated cells are more robust for the mass-conserved version of the equations; see **Figure 8**.

For the original model the speed and shape drastically changes when varying the parameters, and only a particular combination of parameters gives rise to cell crawling (see **Figure 4**). On the other hand, for the new mass-conserved version both velocities and shapes are more similar to each other for a much larger window of parameter values, as we can see in the speeds calculated in **Figure 8**. Such results were obtained by changing k_{18} to correspond to simulations shown in the third row of

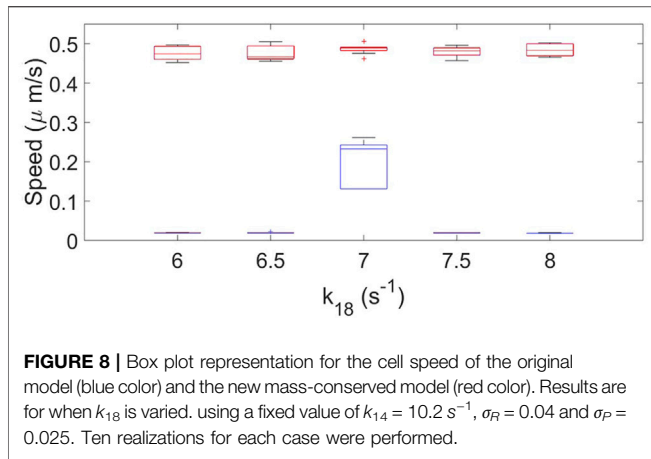


Figure 4 for the no mass conservation case and for **Figure 6** for the mass-conservation system.

In **Figure 9** we show the dependency of the speed on the noise σ_P for different values of σ_R . The speed of the cells employed for the calculation comes from the dynamics shown in **Figures 5, 7**. We observe that the speed obtained from both conditions decreases for greater noise intensities. However, for the original model almost null velocities appear for low noise magnitude. As we increase the noise intensity, values of the speed are more similar.

4 DISCUSSION

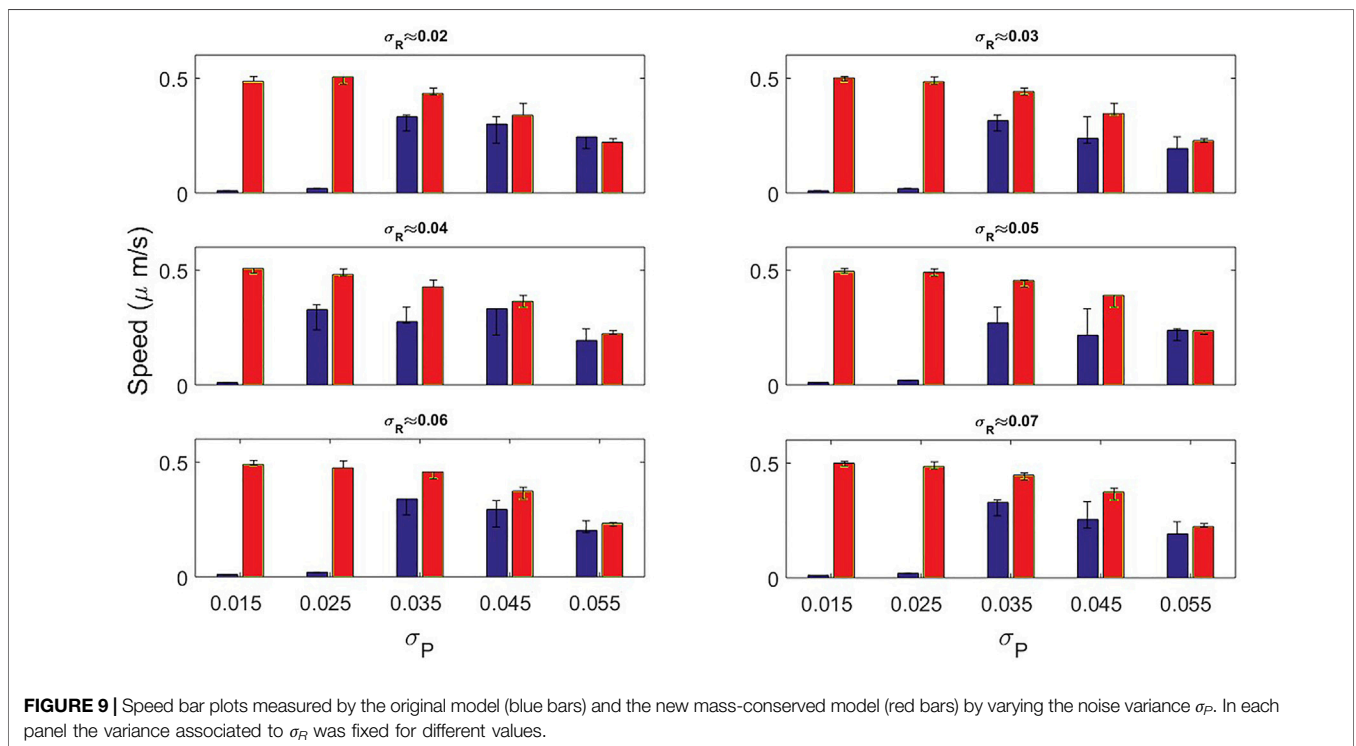
We studied the dynamics of a one-dimensional *Dictyostelium Discoideum* cell model consisting in the stochastic dynamics of

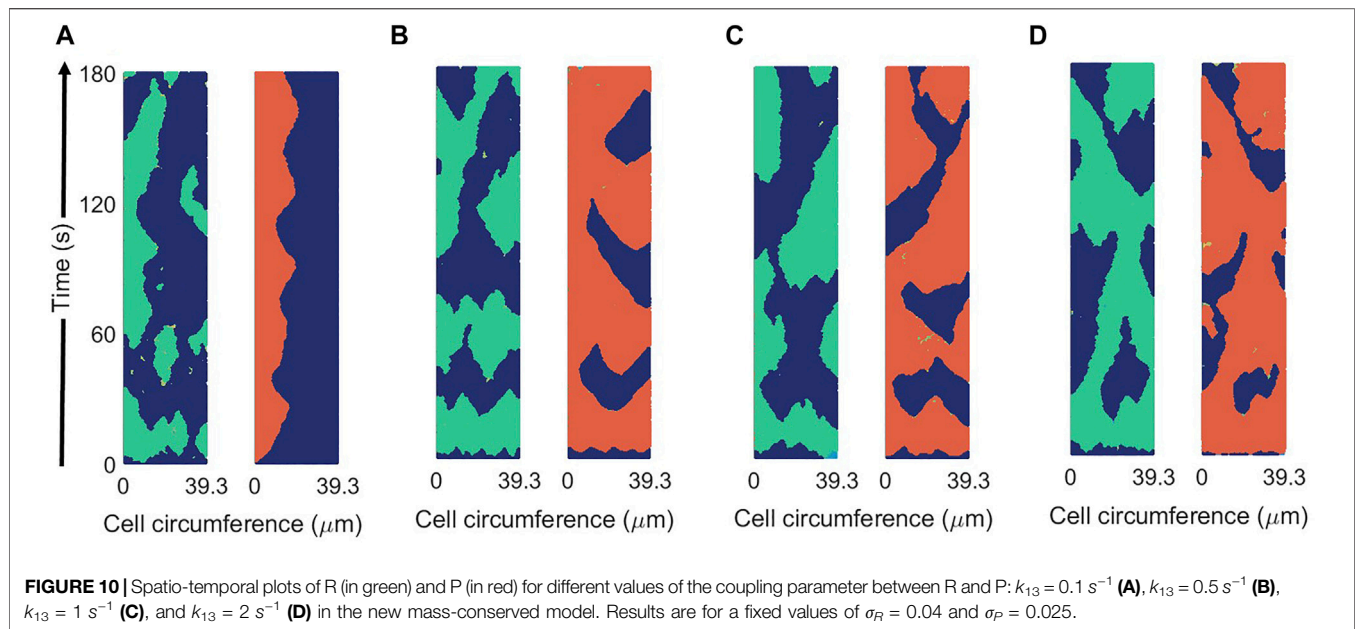
Ras activation (R) and pseudopod inducer (P). The deterministic version of the model reveals the emergence of bistability. This conclusion appears from the visible hysteresis transition under the change of the parameters. In contrast, the stochastic version of the model permits the transition between two stable regimes. The extension of the model into two dimensions with the use of the addition of a phase field, allowing cell deformation, shows similar dependence on the parameters, in agreement with [23].

Since for typical experimental conditions the total concentration barely changes despite environmental perturbations, we chose to incorporate global feedback for the pseudopod inducer inside the cell. Such inclusion increases the robustness of the model and expands the parameter range where cell motion is observed without affecting the shape and dynamics.

The idea behind the approach is to dynamically control the velocity of the border between the clusters of P (orange domains) and the empty region. When the size of the orange domain is above (below) a certain threshold the border contracts (expands) keeping the global size of the domain of P and therefore the polarization of the cell. Such control does not substantially depend on the rest of the parameters because it is defined to maintain the size of the domain close to a certain value, and ensures that small modifications of the parameter do not destroy the structure of the domains and the polarization. Therefore, the described mechanism is more robust than a pure parameter fitting.

A bistable dynamics together with diffusion typically produces the motion of a front in reaction-diffusion equations. Under certain fine tuned parameter values, the front velocity becomes zero [54]. If we consider such bistable variable the concentration at the membrane and we, therefore, couple its dynamics with a





second variable, related with the concentration of the same protein in the cytosol, where diffusion is faster, the condition of zero velocity spontaneously appears, and the front is frozen at a particular position giving rise to wave pinning [13, 29]. Such a pinned condition appears because the coordinated balance between the membrane and the cytosol concentrations maintains constant the total amount of the protein inside the cell. Therefore, some other new models consider only a single variable for the membrane together with a global feedback to account for the mass-conservation condition for a single concentration [17, 32, 38]. When the dynamics of the concentration at the membrane is combined with other membrane concentrations more complex models including also excitable signalling networks are developed [39, 47, 48, 55]. In contrast with such models, in this study we chose an existing complex model where the condition of bistability is finely tuned [23] and add the global feedback condition to account for the conservation of the protein. Such modification highly increases the robustness of the model and, therefore, its applicability to other conditions.

Two of the parameters k_{14} and k_{18} can show hysteresis loops in the concentration of P, see **Figure 3**. We have employed the global feedback in the condition of parameter k_{14} , see **Eq. 9**, however we could have employed a similar condition for parameter k_{18} or any other parameter which exhibits a hysteresis behavior on the concentration P. Actually, note that other global feedback were already considered in the original version of the model [23]; see the dynamics of the global inhibitors, defined by G_R and G_P in **Eqs 2–5** respectively, similarly to other models of the motion of *Dictyostelium discoideum* cells based on global cytosolic quantities [12, 48]. The addition of global control quantities which can determine the available concentration inside the cell has previously been employed in other models [32, 38, 47].

Instant speed was measured, highlighting that for the original model a considerable set of parameters driven to velocities of close to zero, while for the set of parameters for the new mass-conserved model the speed remained almost constant around $0.45 \mu\text{m/s}$.

Note that we have shown that the original model is based on a bistable conditions with the appropriate noise intensity. We have previously used simple stochastic bistable models for the description of the motion of *Dictyostelium discoideum* cells [34, 38] based on the same concept together with a mass-conservation constraint. There are also other models based on similar constraints [24, 40, 47] where some of the key differences relies in the inherent oscillatory dynamics of the models, the specific parameters that need to be change to generate different types of cell motion (e.g., amoeboid or keratocyte) without affecting the biochemical signaling dynamics; apart from the number of membrane concentrations involved in the cell dynamics as already mentioned. Therefore, the addition of a mass conservation constraint is a convenient mechanism to increase robustness in the delicate equilibrium between stochastic fluctuations and a bistable condition.

The coupling of the Ras activation R on the pseudopod inducer P is weak. The coupling is produced by the term proportional to k_{13} and it increases the probability of the generation of patches of P. A chemotactic concentration can enhance R and, therefore, polarize the field P and direct the locomotion [23]. In the absence of chemotaxis the coupling is small, while more physiological conditions may require larger couplings. In **Figure 10** we increased parameter k_{13} to demonstrate the increase in the coupling of both field R and P through the parameter. Intermediate values can be compared with experimental measures to fit an appropriate value; however such evaluation is outside the scope of this work.

An extension of the new mass-conserved model is possible with the inclusion of an external chemo-attractant gradient to analyze the response, known as chemotaxis and already considered in the original model [23]. Future simulations should study the relation of the chemotactic motion of *Dictyostelium discoideum* cells with the stochastic fluctuations and the rest of the parameters. They should also measure the effects on the shape and speed caused by the gradient.

In summary, we have shown that the inclusion of a mass-conservation constraint in the correct position substantially increases the robustness of a computational model of a crawling cell.

DATA AVAILABILITY STATEMENT

The original contributions presented in the study are included in the article/Supplementary Material, further inquiries can be directed to the corresponding author.

REFERENCES

- Cross MC, Hohenberg PC. Pattern Formation outside of Equilibrium. *Rev Mod Phys* (1993) 65:851–1112. doi:10.1103/revmodphys.65.851
- Koch AJ, Meinhardt H. Biological Pattern Formation: from Basic Mechanisms to Complex Structures. *Rev Mod Phys* (1994) 66:1481–507. doi:10.1103/revmodphys.66.1481
- Kondo S, Miura T. Reaction-diffusion Model as a Framework for Understanding Biological Pattern Formation. *science* (2010) 329:1616–20. doi:10.1126/science.1179047
- Gross P, Kumar KV, Goehring NW, Bois JS, Hoeger C, Jülicher F, et al. Guiding Self-Organized Pattern Formation in Cell Polarity Establishment. *Nat Phys* (2019) 15:293–300. doi:10.1038/s41567-018-0358-7
- Kitano H. Biological Robustness. *Nat Rev Genet* (2004) 5:826–37. doi:10.1038/nrg1471
- Whitacre JM. Biological Robustness: Paradigms, Mechanisms, and Systems Principles. *Front Gene* (2012) 3:67. doi:10.3389/fgene.2012.00067
- Mogilner A, Allard J, Wollman R. Cell Polarity: Quantitative Modeling as a Tool in Cell Biology. *Science* (2012) 336:175–9. doi:10.1126/science.1216380
- Camley BA, Rappel W-J. Physical Models of Collective Cell Motility: from Cell to Tissue. *J Phys D: Appl Phys* (2017) 50:113002. doi:10.1088/1361-6463/aa56fe
- Rappel W-J, Edelstein-Keshet L. Mechanisms of Cell Polarization. *Curr Opin Syst Biol* (2017) 3:43–53. doi:10.1016/j.coisb.2017.03.005
- Jilkine A, Edelstein-Keshet L. A Comparison of Mathematical Models for Polarization of Single Eukaryotic Cells in Response to Guided Cues. *Plos Comput Biol* (2011) 7:e1001121. doi:10.1371/journal.pcbi.1001121
- Beta C, Kruse K. Intracellular Oscillations and Waves. *Annu Rev Condens Matter Phys* (2017) 8:239–64. doi:10.1146/annurev-conmatphys-031016-025210
- Xiong Y, Huang C-H, Iglesias PA, Devreotes PN. Cells Navigate with a Local-Excitation, Global-Inhibition-Biased Excitable Network. *Proc Natl Acad Sci U.S.A* (2010) 107:17079–86. doi:10.1073/pnas.1011271107
- Mori Y, Jilkine A, Edelstein-Keshet L. Wave-pinning and Cell Polarity from a Bistable Reaction-Diffusion System. *Biophysical J* (2008) 94:3684–97. doi:10.1529/biophysj.107.120824
- Bergmann F, Zimmermann W. On System-Spanning Demixing Properties of Cell Polarization. *PLoS one* (2019) 14:e0218328. doi:10.1371/journal.pone.0218328
- Brauns F, Halatek J, Frey E. Phase-space Geometry of Mass-Conserving Reaction-Diffusion Dynamics. *Phys Rev X* (2020) 10:041036. doi:10.1103/physrevx.10.041036

AUTHOR CONTRIBUTIONS

EM performed the numerical simulations; EM and SA contributed to the design and implementation of the research, to the analysis of the results and to the writing of the manuscript.

ACKNOWLEDGMENTS

We thank grant PGC2018-095456-B-I00 funded by MCIN/AEI/10.13039/501100011033 and by “ERDF A way of making Europe,” by the “European Union.” E.M. acknowledges also financial support from CONACYT.

SUPPLEMENTARY MATERIAL

The Supplementary Material for this article can be found online at: <https://www.frontiersin.org/articles/10.3389/fphy.2022.881885/full#supplementary-material>

- Halatek J, Frey E. Rethinking Pattern Formation in Reaction-Diffusion Systems. *Nat Phys* (2018) 14:507–14. doi:10.1038/s41567-017-0040-5
- Alonso S, Bär M. Phase Separation and Bistability in a Three-Dimensional Model for Protein Domain Formation at Biomembranes. *Phys Biol* (2010) 7:046012. doi:10.1088/1478-3975/7/4/046012
- Trong PK, Nicola EM, Goehring NW, Kumar KV, Grill SW. Parameter-space Topology of Models for Cell Polarity. *New J Phys* (2014) 16:065009. doi:10.1088/1367-2630/16/6/065009
- Bosgraaf L, Van Haastert PJM. The Ordered Extension of Pseudopodia by Amoeboid Cells in the Absence of External Cues. *PLoS one* (2009) 4:e5253. doi:10.1371/journal.pone.0005253
- Kae H, Lim CJ, Spiegelman GB, Weeks G. Chemoattractant-induced Ras Activation during Dictyostelium aggregation. *EMBO Rep* (2004) 5:602–6. doi:10.1038/sj.embor.7400151
- Etzrodt M, Ishikawa HCF, Dalous J, Müller-Taubenberger A, Bretschneider T, Gerisch G. Time-resolved Responses to Chemoattractant, Characteristic of the Front and Tail of Dictyostelium cells. *FEBS Lett* (2006) 580:6707–13. doi:10.1016/j.febslet.2006.11.031
- Sasaki AT, Janetopoulos C, Lee S, Charest PG, Takeda K, Sundheimer LW, et al. G Protein-independent Ras/PI3K/F-Actin Circuit Regulates Basic Cell Motility. *J Cell Biol* (2007) 178:185–91. doi:10.1083/jcb.200611138
- van Haastert PJM, Keizer-Gunnink I, Kortholt A. Coupled Excitable Ras and F-Actin Activation Mediates Spontaneous Pseudopod Formation and Directed Cell Movement. *MBoC* (2017) 28:922–34. doi:10.1091/mbc.e16-10-0733
- Shi C, Huang C-H, Devreotes PN, Iglesias PA. Interaction of Motility, Directional Sensing, and Polarity Modules Recreates the Behaviors of Chemotaxing Cells. *Plos Comput Biol* (2013) 9:e1003122. doi:10.1371/journal.pcbi.1003122
- Huang C-H, Tang M, Shi C, Iglesias PA, Devreotes PN. An Excitable Signal Integrator Couples to an Idling Cytoskeletal Oscillator to Drive Cell Migration. *Nat Cell Biol* (2013) 15:1307–16. doi:10.1038/ncb2859
- Hecht I, Kessler DA, Levine H. Transient Localized Patterns in Noise-Driven Reaction-Diffusion Systems. *Phys Rev Lett* (2010) 104:158301. doi:10.1103/physrevlett.104.158301
- Hecht I, Skoge ML, Charest PG, Ben-Jacob E, Firtel RA, Loomis WF, et al. Activated Membrane Patches Guide Chemotactic Cell Motility. *Plos Comput Biol* (2011) 7:e1002044. doi:10.1371/journal.pcbi.1002044
- Neilson MP, Veltman DM, van Haastert PJM, Webb SD, Mackenzie JA, Insall RH. Chemotaxis: a Feedback-Based Computational Model Robustly Predicts Multiple Aspects of Real Cell Behaviour. *Plos Biol* (2011) 9:e1000618. doi:10.1371/journal.pbio.1000618

29. Otsuji M, Ishihara S, Co C, Kaibuchi K, Mochizuki A, Kuroda S. A Mass Conserved Reaction-Diffusion System Captures Properties of Cell Polarity. *Plos Comput Biol* (2007) 3:e108. doi:10.1371/journal.pcbi.0030108
30. Camley BA, Zhao Y, Li B, Levine H, Rappel W-J. Periodic Migration in a Physical Model of Cells on Micropatterns. *Phys Rev Lett* (2013) 111:158102. doi:10.1103/physrevlett.111.158102
31. Shao D, Levine H, Rappel W-J. Coupling Actin Flow, Adhesion, and Morphology in a Computational Cell Motility Model. *Proc Natl Acad Sci U.S.A* (2012) 109:6851–6. doi:10.1073/pnas.1203252109
32. Camley BA, Zhao Y, Li B, Levine H, Rappel WJ. Crawling and Turning in a Minimal Reaction-Diffusion Cell Motility Model: Coupling Cell Shape and Biochemistry. *Phys Rev E* (2017) 95:012401. doi:10.1103/PhysRevE.95.012401
33. Nickaen M, Novak IL, Pulford S, Rumack A, Brandon J, Slepchenko BM, et al. A Free-Boundary Model of a Motile Cell Explains Turning Behavior. *Plos Comput Biol* (2017) 13:e1005862. doi:10.1371/journal.pcbi.1005862
34. Alonso S, Stange M, Beta C. Modeling Random Crawling, Membrane Deformation and Intracellular Polarity of Motile Amoeboid Cells. *PloS one* (2018) 13:e0201977. doi:10.1371/journal.pone.0201977
35. Stankevics L, Ecker N, Terriac E, Maiuri P, Schoppmeyer R, Vargas P, et al. Deterministic Actin Waves as Generators of Cell Polarization Cues. *Proc Natl Acad Sci U.S.A* (2020) 117:826–35. doi:10.1073/pnas.1907845117
36. Ecker N, Kruse K. Excitable Actin Dynamics and Amoeboid Cell Migration. *Plos one* (2021) 16:e0246311. doi:10.1371/journal.pone.0246311
37. Miao Y, Bhattacharya S, Edwards M, Cai H, Inoue T, Iglesias PA, et al. Altering the Threshold of an Excitable Signal Transduction Network Changes Cell Migratory Modes. *Nat Cel Biol* (2017) 19:329–40. doi:10.1038/ncb3495
38. Moreno E, Flemming S, Font F, Holschneider M, Beta C, Alonso S. Modeling Cell Crawling Strategies with a Bistable Model: From Amoeboid to Fan-Shaped Cell Motion. *Physica D: Nonlinear Phenomena* (2020) 412:132591. doi:10.1016/j.physd.2020.132591
39. Cao Y, Ghabache E, Miao Y, Niman C, Hakoziaki H, Reck-Peterson SL, et al. A Minimal Computational Model for Three-Dimensional Cell Migration. *J R Soc Interf* (2019) 16:20190619. doi:10.1098/rsif.2019.0619
40. Cao Y, Ghabache E, Rappel WJ. Plasticity of Cell Migration Resulting from Mechanochemical Coupling. *Elife* (2019) 8:e48478. doi:10.7554/eLife.48478
41. Moure A, Gomez H. Phase-field Model of Cellular Migration: Three-Dimensional Simulations in Fibrous Networks. *Comput Methods Appl Mech Eng* (2017) 320:162–97. doi:10.1016/j.cma.2017.03.025
42. Flemming S, Font F, Alonso S, Beta C. How Cortical Waves Drive Fission of Motile Cells. *Proc Natl Acad Sci U.S.A* (2020) 117:6330–8. doi:10.1073/pnas.1912428117
43. Löber J, Ziebert F, Aranson IS. Collisions of Deformable Cells lead to Collective Migration. *Scientific Rep* (2015) 5:9172.
44. Kulawiak DA, Camley BA, Rappel W-J. Modeling Contact Inhibition of Locomotion of Colliding Cells Migrating on Micropatterned Substrates. *Plos Comput Biol* (2016) 12:e1005239. doi:10.1371/journal.pcbi.1005239
45. Moreno E, Grossmann R, Beta C, Alonso S. From Single to Collective Motion of Social Amoebae: A Computational Study of Interacting Cells. *Front Phys* (2022) 9:750187. doi:10.3389/fphys.2021.750187
46. Kitano H. Towards a Theory of Biological Robustness. *Mol Syst Biol* (2007) 3:137. doi:10.1038/msb4100179
47. Imoto D, Saito N, Nakajima A, Honda G, Ishida M, Sugita T, et al. Comparative Mapping of Crawling-Cell Morphodynamics in Deep Learning-Based Feature Space. *Plos Comput Biol* (2021) 17:e1009237. doi:10.1371/journal.pcbi.1009237
48. Taniguchi D, Ishihara S, Oonuki T, Honda-Kitahara M, Kaneko K, Sawai S. Phase Geometries of Two-Dimensional Excitable Waves Govern Self-Organized Morphodynamics of Amoeboid Cells. *Proc Natl Acad Sci U.S.A* (2013) 110:5016–21. doi:10.1073/pnas.1218025110
49. Cooper RM, Wingreen NS, Cox EC. An Excitable Cortex and Memory Model Successfully Predicts New Pseudopod Dynamics. *PloS one* (2012) 7:e33528. doi:10.1371/journal.pone.0033528
50. van Haastert PJM. Short- and Long-Term Memory of Moving Amoeboid Cells. *PloS one* (2021) 16:e0246345. doi:10.1371/journal.pone.0246345
51. García-Ojalvo J, Sancho J. *Noise in Spatially Extended Systems*. Berlin, Germany: Springer Science & Business Media (2012).
52. Hanggi P, Mroczkowski TJ, Moss F, McClintock PVE. Bistability Driven by Colored Noise: Theory and experiment. *Phys Rev A* (1985) 32:695–8. doi:10.1103/physreva.32.695
53. Kramers HA. Brownian Motion in a Field of Force and the Diffusion Model of Chemical Reactions. *Physica* (1940) 7:284–304. doi:10.1016/s0031-8914(40)90098-2
54. Beta C, Amselem G, Bodenschatz E. A Bistable Mechanism for Directional Sensing. *New J Phys* (2008) 10:083015. doi:10.1088/1367-2630/10/8/083015
55. Saito N, Sawai S. Three-dimensional Morphodynamic Simulations of Macropinocytic Cups. *Science* (2021) 24:103087. doi:10.1016/j.isci.2021.103087

Conflict of Interest: The authors declare that the research was conducted in the absence of any commercial or financial relationships that could be construed as a potential conflict of interest.

Publisher's Note: All claims expressed in this article are solely those of the authors and do not necessarily represent those of their affiliated organizations, or those of the publisher, the editors and the reviewers. Any product that may be evaluated in this article, or claim that may be made by its manufacturer, is not guaranteed or endorsed by the publisher.

Copyright © 2022 Moreno and Alonso. This is an open-access article distributed under the terms of the Creative Commons Attribution License (CC BY). The use, distribution or reproduction in other forums is permitted, provided the original author(s) and the copyright owner(s) are credited and that the original publication in this journal is cited, in accordance with accepted academic practice. No use, distribution or reproduction is permitted which does not comply with these terms.